Two-branch break-up systems by a single mantle plume: Insights from numerical modeling

Anouk Beniest, Alexander Koptev, Sylvie Leroy, William Sassi, Xavier Guichet

Two-branch break-up systems by a single mantle plume:

Insights from numerical modeling

Running title: Two-branch break-up systems by single plume

A. Beniest[1, 2], A. Koptev.[1,3], S. Leroy,[1], W. Sassi[2], X. Guichet[2]

[1]Sorbonne Universités, UPMC University Paris 06, ISTeP, CNRS-UMR 7193, Paris, France

[2]IFP Energies nouvelles, Geosciences Division, Rueil-Malmaison, France

[3] Now at Department of Geosciences, University of Tübingen, Tübingen, Germany

Corresponding author: Anouk Beniest (anouk.beniest@etu.upmc.fr)

Key Points:

- A single mantle plume can be responsible for two non-contemporaneous rift-to-spreading systems in a laterally non-homogeneous lithosphere
- The pre-rift distance between a plume and a lateral lithospheric boundary between two segments controls rift-to-spreading systems
- The location of a plume with respect to lithosphere inhomogeneities is a key-variable when modeling plume-induced continental break-up

Abstract

Thermo-mechanical modeling of plume-induced continental break-up reveals that the initial location of a mantle anomaly relative to a lithosphere inhomogeneity has a major impact on the geometry and timing of a rift-to-spreading system. Models with a warmer Moho temperature are more likely to result in 'plume-centered' mode, where the rift and subsequent spreading axis grow directly above the plume. Models with weak far-field forcing are inclined to develop a 'structural inherited' mode, with lithosphere deformation localized at the lateral lithospheric boundary. Models of a third group cultivate two break-up branches (both 'plume-centered' and 'structural inherited') that form consecutively with a few million years delay. With our experimental setup, this break-up mode is sensitive to relatively small lateral variations of the initial anomaly position. We argue that one single mantle anomaly can be responsible for non-simultaneous initiation and development of two rift-to-spreading systems in a lithosphere with a lateral strength contrast.

1. Introduction

Continental rifting is a complex process that depends on many factors such as the rheological structure of the crust and lithospheric mantle [*Brun*, 2002; *Burov*, 2011], thermal distribution in the lithosphere [*Lavier and Manatschal*, 2006; *Brune et al.*, 2014]), the presence or absence of inherited structures [*Chenin and Beaumont*, 2013; *Manatschal et al.*, 2015], far-field forces [e.g. *Huismans et al.*, 2001] and mantle plume(s) [*Burov and Gerya*, 2014]. To date, a variety of analogue and numerical models have examined plume-induced continental rifting and break-up. For example, these models are able to explain quite complex geometries of a plume itself [*Davaille et al.*, 2005] and its diverse effects when interacting with a rheologically stratified lithosphere such as asymmetric short-wavelength topography [*Burov and Cloetingh*, 2010; *Burov and Gerya*, 2014], the reduction of lithospheric strength [*Brune et al.*, 2013], the multiphase development of rifting with a quick transition from wide to narrow mode [*Koptev et al.*, 2017] and the

shifted position of the break-up center with respect to the initial point of plume impingement [*Beniest et al.*, 2017].

Single rift – plume interactions are well-investigated, but complex multi-branch continental rift and oceanic spreading systems are less well-understood even though they exist all around the world. The Labrador Sea between Greenland and mainland Canada [*Chalmers et al.*, 1995; *Saunders et al.*, 1997] and the Aegir Ridge between Greenland and Norway [*Gaina et al.*, 2009] are two (non-active) spreading branches that developed consecutively in the North Atlantic region (Fig. 1a, for tectonic reconstruction see *Skogseid et al.* [2000]). The Abimael Ridge offshore south Brazil (Fig. 1b, for tectonic reconstruction see e.g. *Torsvik et al.* [2009] and *Moulin et al.* [2010]) corresponds to an abandoned part of the South Atlantic rift system [*Mohriak et al.*, 2010]. Another example is the Tasman Sea that is separated by the Dampier Ridge from the Lord Howe Rise and Middleton Basin, all part of the same rift system (Fig. 1c, for tectonic reconstruction see *Gaina et al.* [1998]). These ridges and branches differ significantly in terms of the width of newly formed oceanic lithosphere and the distance between active and aborted ridges. For example, the total width of the Norwegian-Greenland Sea reaches for some 1000 km (Fig. 1a, [*Greenhalgh and Kusznir*, 2007]) whereas both the Labrador and Tasman Sea only gained 100 of km's of oceanic crust width before abortion (Fig. 1a and 1c). The oceanic lithosphere associated with the Abimael ridge is even narrower than the Labrador Sea and the Tasman Sea, with a total width of a couple of 10's of kilometers only (Fig. 1b, [*Mohriak et al.*, 2010]). The Lord Howe Rise and Middleton Basin (Fig. 1c) have only reached a rift phase (between 90 Ma and 84 Ma, *Gaina et al.* [1998]), not providing any evidence for oceanic crust formation, but they remain a separate branch of the break-up system of the Tasman Sea, where spreading initiated at 83 Myr [*Gaina et al.*, 1998]. The distance between the present-day location of the aborted and active rift- and spreading ridges can be as far away as over 5000 km's in the case of the Abimael ridge and the South Atlantic mid-ocean ridge (Fig. 1b) or as close by as only 200 km in case of the Aegir Ridge (Fig. 1a). Despite these differences, such multi-branch systems have one important thing in common: they are underlain by a deep-rooted mantle anomaly with varying geometries that may have triggered their initiations and controlled their subsequent evolution. Present-day geometries of mantle anomalies can be visualized with mantle tomography. This

method suggests that the Iceland plume (Fig.1a, after [*Zhao*, 2007]) extends throughout the mantle to the core-mantle boundary [*French and Romanowicz*, 2015]. The Tristan plume (Fig.1b, [*Zhao*, 2007]) is rooted in the lower mantle and seems to be failing in the upper mantle nowadays, although it leaves an ancient hotspot trail behind [*Schlömer et al.*, 2017]. The Tasmantid (TasP) low velocity zone (Fig.1c, [*Zhao*, 2007]) is currently confined to the upper mantle and transition zone with a lower mantle stem significantly distanced from the upper mantle part of the plume. Yet, up to five ancient hotspots could be the surface expressions of this mantle plume [*Davies et al.*, 2015].

Despite numerous numerical modeling exercises [*Huismans and Beaumont*, 2008; *Chenin and Beaumont*, 2013; *Brune et al.*, 2014; *Burov and Gerya*, 2014; *Koptev et al.*, 2016; *Beniest et al.*, 2017; *Lavecchia et al.*, 2017] no self-consistent numerical model has thus far explained how multi-branch break-up centers, separated in space and time, can result from the impact of the same mantle plume (Fig. 1). Here, we present the results of a 2D thermo-mechanical modeling study investigating the effect of the pre-rift position of a mantle plume anomaly on the rift-to-spreading evolution in a laterally heterogeneous lithosphere, with different initial Moho temperatures and various extension rates.

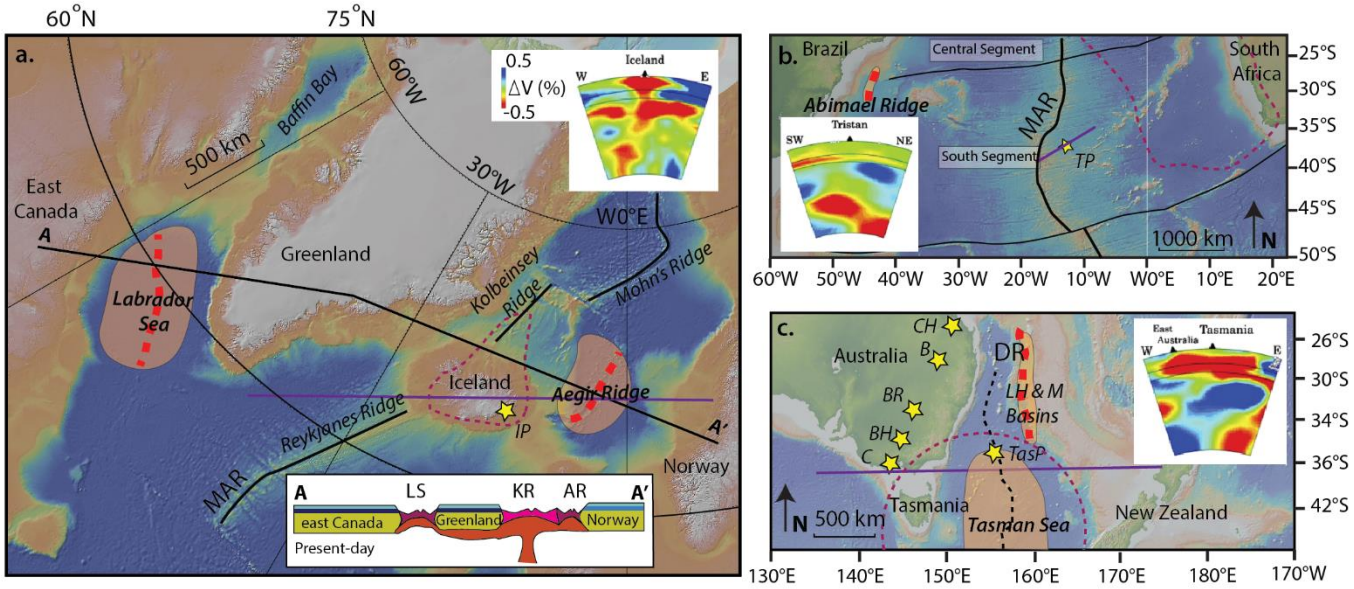

Figure 1. Three natural examples of a complex multi-branch spreading system associated with a single mantle plume: a) The Labrador Sea [*Chalmers et al.*, 1995] and the Aegir Ridge [*Greenhalgh and Kusznir*,

2007] developed consecutively in the North Atlantic region. The Iceland plume (dashed purple line) is now located directly below currently active mid-ocean ridge (Rickers et al., 2013). The black line represents a position of a schematic cross-section of the North Atlantic domain (for color-code see Figs. 2 and 4). b) The Abimael Ridge is a failed rift branch along which evidence for oceanic crust has been observed (e.g. Mohriak et al., 2010). The Tristan Plume associated to the African Superswell (dashed purple line) is located close to the South Atlantic mid-ocean ridge [*Ernesto et al.*, 2002]. c) The spreading axes of the Tasman Sea and rift axis of Lord Howe and Middleton Basins are part of the same system [*Gaina et al.*, 1998]. The Tasmantid (TasP) and Cosgrove (C) hotspots lay on the edge of the Tasmantid Plume (dashed purple line). The tomographic images are taken from Zhao [2007]. The purple lines show their approximate location. The yellow stars are asthenosphere hotspot locations. *IP = Iceland Plume hotspot, LS = Labrador Sea, KR = Kolbeinsey Ridge, AR = Aegir Ridge, MAR = Mid-Atlantic Ridge, TP = Tristan Plume hotspot, BH = Begargo Hill hotspot, BR = Bokhara River hotspot, B = Buckland Hotspot, CH = Cape Hillsborough hotspot, DR = Dampier Ridge, LH&M Basins = Lord Howe and Middleton Basins. Australian hotspots after Davies et al. [2015].*

2. Numerical model setup

We use a 2D version of the viscous-plastic numerical code I3ELVIS [*Gerya and Yuen*, 2007] to study plume-induced rifting and continental break-up of a lithosphere with a lateral rheological contrast. This code combines a finite difference method on a staggered Eulerian grid with a marker-in-cell technique. For a detailed description of the code we refer to *Gerya and Yuen* [2007], *Gerya* [2010] and supplementary material 1.

The spatial dimensions of the model are 1500 km in length and 635 km in width. The model box contains 297 x 133 nodes, so that the grid cell size corresponds to 5 x 5 km. The model setup consists of a three-layered lithosphere (150 km), overlying the sublithospheric mantle (455 km). The crustal thickness is 40 km, equally divided in upper crust (20 km) and lower crust (20 km) (supplementary Fig. 1.1). The homogenous upper crust has ductile properties of wet quartzite whereas the lower crust is characterized by

a lateral contrast in rheological strength: a 'strong' left side, made of anorthite rheology, and a 'weak' right side, consisting of wet quartzite rheology [*Bittner and Schmeling*, 1995; *Clauser and Huenges*, 1995; *Kohlstedt et al.*, 1995; *Ranalli*, 1995; *Turcotte and Schubert*, 2002; *Connolly*, 2005]. The contact between these two rheologically different crustal segments represents a simplified inherited structure, located in the top-middle of the model box. The lithospheric and sublithospheric mantle uses dry olivine rheology whereas the mantle plume is simulated with wet olivine rheology (more detailed information on rheological and material properties of the crust can be found in supplementary table 2.1). The initial mantle plume anomaly is positioned at the base of the model box and has a spherical shape with a radius of 200 km, which is in correspondence with previous work [e.g. *Burov and Gerya, 2014; Koptev et al.*, 2015]. We use a linear geotherm with 0 ^{o}C at the surface, 500 ^{o}C or 600 ^{o}C at the Moho (40 km), 1300 ^{o}C at the base of the lithosphere (150 km) and 1630 ^{o}C at the bottom of the model domain (635 km). The Moho temperature (500 ^{o}C and 600 ^{o}C) is one of the variable parameters of our study (supplementary table 3.1). The mantle anomaly has an initial temperature of 2000 ^{o}C corresponding to 300-370 ^{o}C contrast with surrounding mantle. The general thermal boundary conditions align with fixed temperatures at the top (0 ^{o}C) and bottom (1630 ^{o}C) of the model and zero heat flux is imposed on the vertical boundaries of the model box. Far-field tectonic extension is applied on both vertical sides with a constant half-rate of 5 mm/yr or 10 mm/yr (supplementary table 3.1). The resulting horizontal forces along the border of the models are of the same order of magnitude ($5x10^{12}$ N per unit length) as "ridge push" [e.g. *Buck*, 2007] and "slab-pull" forces [*Schellart*, 2004]. Apart from the initial Moho temperature and the initial extension rate, our main changing parameter is the pre-rift plume location. In a previous study of *Beniest et al.* [2017] the anomaly was positioned at three different locations with respect to the crustal rheological and geometrical variations. For this study, the mantle plume is initially placed directly below the rheological contact after which it is positioned further away from this contact below the 'stronger' half of the model with steps of 25-100 km. The maximum lateral shift of the plume with respect to its central location is 450 km. We performed 3 sets of 9 numerical experiments, resulting in 27 models total (supplementary table 3.1). The first set has a Moho temperature of 500 ^{o}C and an extension rate of 10 mm/yr, the second set has a Moho temperature of 600 ^{o}C and an extension rate of

10 mm/yr and the last set has a Moho temperature of 500 ^{o}C and an extension rate of 5 mm/yr. In addition, we performed 19 complementary models (supplementary material 3.2 and 4) to test the models sensitivity to certain parameters such as grid cell size (higher resolution), plume size (larger radius), plume temperature (1900 ^{o}C instead of 2000 ^{o}C), Moho isotherm (650 ^{o}C) and more complex structure of the lithospheric mantle (different thicknesses for "stronger" and "weaker" segments) and crustal geotherm (non-linear).

3. Experimental results

In all models the mantle plume rises rapidly, reaching the base of the lithosphere in less than 2 Myr. Plume material spreads laterally along the lowest part of the lithosphere flowing as far away as ~1000 km (similarly to previous 2D experiments of *Burov and Cloetingh* [2010] and 3D models of *Koptev et al.* [2017]). Unlike these models, our experiments develop different rift-to-break-up modes that can be divided into three major groups (Fig. 2 and supplementary table 3.1).

The first group demonstrates continental break-up directly above the initial plume location ('plume-centered' break-up mode, model 8, Fig. 2d and supplementary Fig. 5.1d). This category corresponds to the classical plume models also shown by e.g. *d'Acremont et al.* (2003) and *Burov and Cloetingh* [2010]. Despite initial deformation localization at the contact between the 'weak' and 'strong' segments ('structural inherited') (supplementary Fig. 5.1d; 1 Myr), vertical ascent of hot plume material throughout the lithospheric mantle (Fig. 2d; 10 Myr) leads to a second 'plume-centered' zone of localized strain (supplementary Fig. 5.1d; 10 Myr). This zone becomes the dominant deformation domain (supplementary Fig. 5.1d; 13 Myr) at the moment of the continental break-up (Fig. 2d; 13 Myr). The initial 'structural' inherited' deformation zone becomes eventually completely extinct (supplementary Fig. 5.1d; 21 Myr). Thus, the plume material flowing laterally at the base of the lithosphere is unable to turn the distant 'structural inherited' rifting into a break-up center (supplementary Fig. 5.1d).

The second category includes models showing rifting and subsequent break-up only at the contact between two rheological segments ('structural inherited' break-up mode). Here, due to the initial plume position being closer to the inherited structure, localized plume ascent coincides with the 'structural inherited' zone

160 of the initial continental rifting. This leads to plume-induced (but 'structural inherited') break-up (model 3,
161 Fig. 2a). Note that there is no evidence for strain localization within the stronger lithosphere above the initial
162 plume location (supplementary Fig. 5.1a).
163 Models of the third group illustrate an intermediate behavior where two break-up centers form
164 consecutively. These 'two-branch' experiments develop first the 'structural inherited' and then the 'plume-
165 centered' break-up modes or vice-versa depending on the initial plume position (models 6 and 7, Figs. 2b
166 and 2c). In both cases the first rifting phase is 'structural inherited' (supplementary Figs. 5b-c; 1 Myr), but
167 the order in which the break-up centers develop, depends heavily on relatively small (< 30 km) lateral
168 variation of the initial plume position with respect to the rheological boundary (Figs. 2b-c and
169 supplementary Figs. 5b-c). When the initial thermal anomaly is situated further away from the rheological
170 contact (at 375 km) 'plume-centered' break-up develops first, directly above the anomaly. This is due to the
171 rapid, localized ascent of plume material through the mantle part of the stronger overlying lithosphere (Fig.
172 2c and supplementary Fig. 5.1c, 11-16 Myr). After that, hot plume material residing at the base of the
173 lithosphere rises below the 'structural inherited' rift zone (Fig. 2c and supplementary Fig. 5.1c; 16 Myr)
174 leading to complete rupture of the continent at the pre-imposed structural boundary (Fig. 2c and
175 supplementary Fig. 5.1c; 22 Myr). When the mantle plume is positioned only 350 km away from the
176 rheological contact 'structural inherited' break-up develops first, followed by a 'plume-centered' one (Fig.
177 2b; supplementary Fig. 5.1b). In both cases the time delay between these two continental break-ups is less
178 than 10 Myr.
179

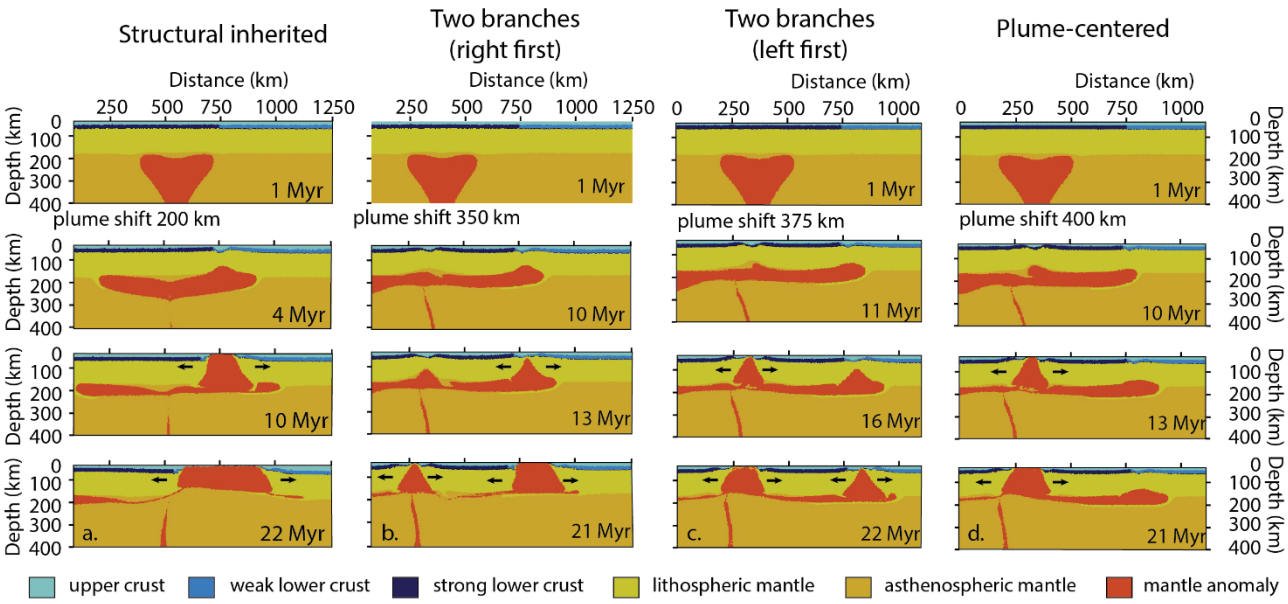

Figure 2. The most representative examples of the three different break-up modes (from the model series distinguished with a Moho temperature of 500 °C and half-rate extension of 10 mm/yr, see also Fig. 3a and supplementary table 3.1): a) model 3 with an initial plume shift towards the stronger segment of 200 km: "structural inherited" mode; b-c) models 6 (plume shift of 350 km) and model 7 (plume shift of 375 km): "two-branch" mode; d) model 8 (plume shift of 400 km): "plume-centered" mode. Note that not only the initial position but also the initial size (models 37-38) and temperature (models 39-42) of the mantle anomaly (supplementary Figs. 4.3 and 4.4) might be critical for the final break-up mode.

The 'two-branch' category results from the reference model setup that uses a relatively fast extension rate (half-rate 10 mm/yr) and colder Moho temperature (500 °C, models 1-9, Fig. 3a). In a different set of models where the extension rate is being kept at 10 mm/yr but the crustal geotherm is warmer (600 °C at the Moho, models 10-18), a similar 'two-branch' system is produced when the plume is shifted 300 km away from the rheological contact (Fig. 3b). Note, however, that in this model only the 'plume-centered' rift axis evolves into a spreading center, whereas the 'structural inherited' branch does not reach this phase. For this set of model setups, the 'plume-centered' break-up mode is the dominant break-up mechanism when the anomaly is located 350 km or further away from the inherited structure (Fig. 3b). A series of complementary

197 experiments show that a further increase in the initial crustal geotherm (e.g. 650 ^{o}C, models 30-36) has no
198 principal effect on the final continental break-up mode (compare Fig. 3b and supplementary Fig. 4.2). Small
199 variations in the initial temperature distribution, e.g. a non-linear crustal geotherm that takes into account
200 radiogenic heat production (model 29, supplementary Fig. 4.1c), does not play a significant role neither. For
201 the last set of models the thermal state is the same as for the reference model (500 ^{o}C Moho temperature)
202 and the spreading rate is decreased to 5 mm/yr half-rate extension (models 19-27). For this model series, all
203 models persistently cultivate 'structural inherited' break-up for all tested mantle plume emplacements (Fig
204 3c). Exactly the same behavior is observed in the complementary experiments that include non-uniform
205 thicknesses of the lithosphere with a thicker "stronger" (150 km) segment and a thinner "weaker" (100 km)
206 segment (models 43-46). Regardless the initial plume position and the type of transitional zone between the
207 different rheological segments (vertical or slope), these models show only "structural inherited" break-up
208 mode, without any evidence for "plume centered" rift initiation (supplementary Fig. 4.5). Without
209 dismissing that such contrasts in the rheological and thermal structure are present not only at crustal level
210 but also in the lithospheric mantle, our results provide new elements to evaluate the importance of the mantle
211 inhomogeneities on the initiation and development of multi-branch rift systems.

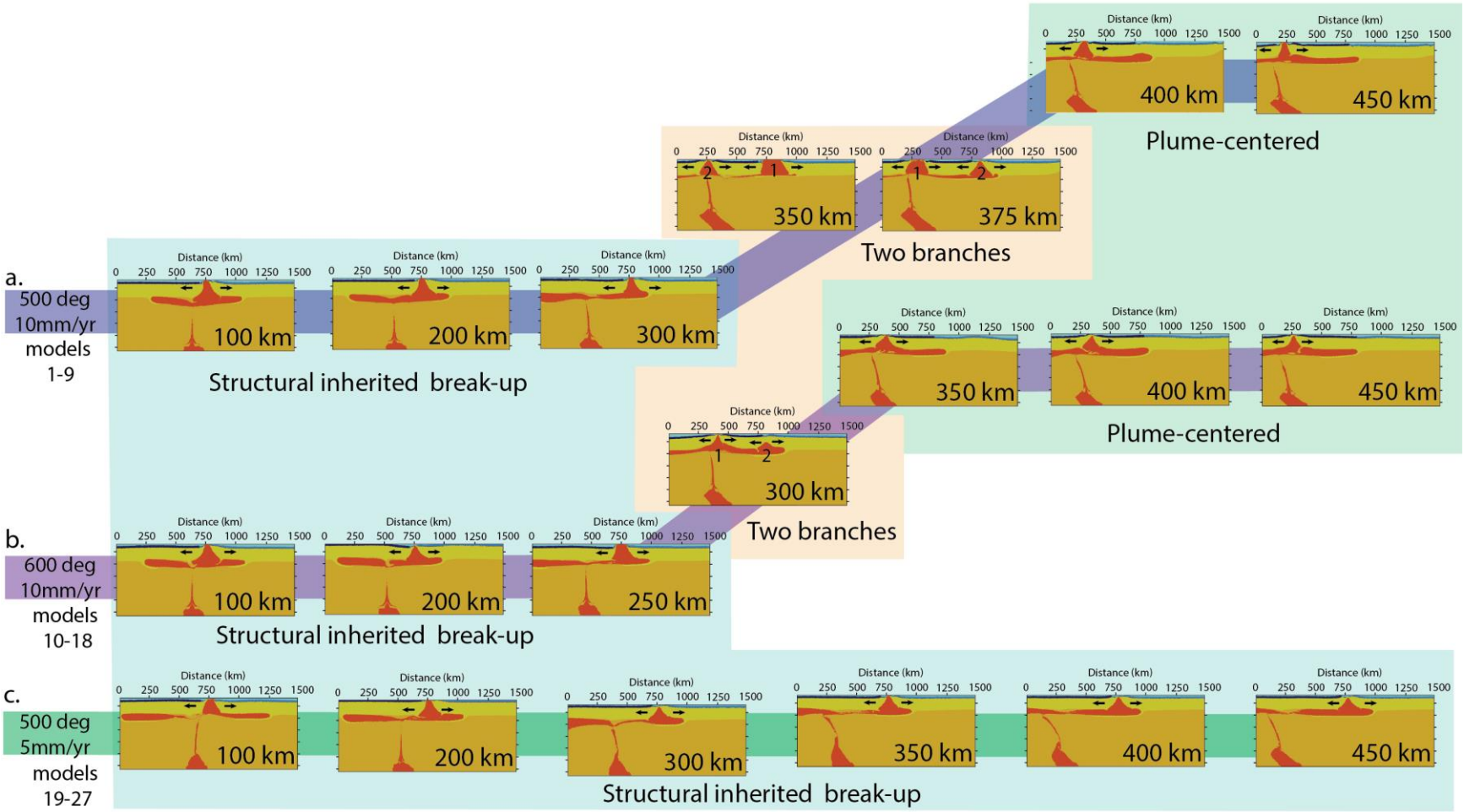
a.
500 deg
10mm/yr
models
1-9
Distance (km)
100 km
200 km
300 km
Structural inherited break-up
350 km
375 km
Two branches
400 km
450 km
Plume-centered
b.
600 deg
10mm/yr
models
10-18
250 km
c.
500 deg
5mm/yr
models
19-27

Figure 3. Graph showing the results of the three sets of models (a. 500 °C Moho temperature and 10 mm/yr extension rate, b. 600 °C Moho temperature and 10 mm/yr extension rate and c. 500 °C Moho temperature and 5 mm extension rate) aligned with increasing distance between the initial anomaly location and the rheological contact. For the experiments with faster extension half-rate (10 mm/yr) there is a critical distance when the system changes from "structural inherited" to "plume-centered" break-up through a two-branch system. This distance is between 300 and 400 km for the Moho temperature of 500 °C (a) and between 250 and 350 km for Moho temperature of 600 °C (b). Closer to the rheological boundary the rift-to-spreading system develops uniquely above the structural inheritance, further away it evolves directly above the plume impingement point. Note that "plume-centered" mode of development does not exclude some localization of initial deformation at the rheological contact ("structural inherited" aborted rifting, see supplementary Fig. 5.1).

4. Discussion and conclusion

Our results show that in case of a cold Moho (500 °C) and relatively fast (10 mm/yr) extension, three modes of break-up are possible, depending on the location of the mantle anomaly with respect to a rheological contact. With respect to this "reference model" set, a higher Moho temperature better facilitates deeper penetration of plume material into the lithosphere. This favors a vertical localized ascent up to the Moho ultimately leading to continental break up directly above initial plume emplacement. This "plume-centered" axis is situated closer to the rheological contact than in case of lower Moho temperature. A general example of this 'plume-centered' rifting, can be observed in for example the Afar depression where the formation of complex triple junction [e.g. *McClusky et al.*, 2010] is linked to the arrival of the Afar plume [*Bellahsen et al.*, 2003] at ~30 Ma [*Hofmann et al.*, 1997; *Coulié et al.*, 2003]. In case extension rate is relatively low (5 mm/yr extension), the thermal impact of the mantle plume becomes less important, the system prefers deformation localization at the mechanical instability created by the rheological contact. This implies that external tectonic forcing is too weak to localize deformation outside of the pre-defined structural boundary

even in presence of an active mantle anomaly that is considerably shifted with respect to this structure. This is generally consistent with numerical results done by *Burov and Gerya* [2014].

A natural example for 'structural inherited' break-up could be the South Atlantic domain where plume-induced break-up takes place at the boundary between stronger (African) and weaker (South-American) lithosphere segments despite possible eastward offset initial position of the mantle plume with respect to this boundary (see *Beniest et al.*, [2017] for more details).

When the anomaly is located at a position where both the impact of the mantle anomaly on the lithosphere and the predefined rheological contact of the system are competing for deformation localization, the 'two-branch' break-up mode develops. For our reference models set (Fig. 3a), a 'two-branch' system forms when the mantle anomaly has a lateral displacement of 350-375 km towards the stronger half of the model domain with respect to the rheological contact. The two branches develop consecutively, with roughly 10 Myr delay, with either 'structural inherited' break-up first, followed by 'plume-centered' (displacement 350 km, Fig. 2b) or the other way around (displacement 375 km, Fig. 2c). Slight offset to this specific dislocation converts the break-up mode to either 'structural inherited' or 'plume-centered' (Figs. 2 and 3).

Both "plume-centered" and "structural inherited" modes of break-up have been modelled by *Beniest et al.*, [2017] and *Lavecchia et al.*, [2017]. To model a "two-branch" system a particular position of the mantle plume anomaly with respect to rheological contrast at the crustal level should be determined. Only relatively narrow (25-50 km) range of initial plume locations can result in multi-branch systems associated with the direct impact of locally upwelled plume material. The thermal state appears to be of lesser importance (see Fig. 3a-b where two branches develop with both colder and hotter Moho temperatures), but far-field forcing should not be too weak (see Fig.3c). Our 'two-branch' model with a plume location 375 km away from the rheological contact bears most similarities to the geodynamic history of the North Atlantic region (Fig. 4). Here, the old and rigid lithosphere of the Greenland craton [*Kerr et al.*, 1997] was underlain by a single mantle anomaly (the Iceland mantle plume) before rifting started in the Labrador Sea [*Lundin and Doré*, 2002; *Rogozhina et al.*, 2016]. The old craton was subjected to plume-activated continental rifting in the Late Triassic or Jurassic followed by seafloor spreading with the oldest accepted magnetic anomaly being

of Danian (~64 Ma) age [*Chalmers et al.*, 1995] (although older anomalies are still a matter of debate [*Peace et al.*, 2016]). Note, however, that the opening of the mostly amagmatic Labrador Sea might have started before the mantle plume impacted the lithosphere beneath West Greenland [Larsen and Saunders, 1998]. A second axis of active spreading (the Aegir ridge) initiated at 57 Ma (i.e. 5-10 Myrs later) [*Lundin and Doré*, 2002] close to the adjacent Caledonian suture zone [*Gaina et al.*, 2009; *Abdelmalak et al.*, 2016], several 100's of kilometers away from the area of the first plume impingement. Thus, both the position of the Iceland plume (e.g. *Rogozhina et al.* [2016] and references herein) near the western coast of Greenland (with a shift of several hundreds of kilometers with respect to the weaker Caledonian suture) at the moment of the initiation of the first spreading branch (even if the paleo-position of the Iceland hotspot remains debatable – see e.g. [*Torsvik et al.*, 2015]) and the time delay of less than 10 Myr between "plume-induced" and "structural inherited" break-ups bear strong similarity with the key features of our "two-branch" model displayed in Fig. 2c and Fig. 4a-c. In this case, the key-features refer to 1) lateral varying rheological contact resembling an inherited structure (the Caledonian Suture), 2) a relatively cool thermal structure comparable to a craton (West-Canada-Greenland craton), 3) the location of the mantle anomaly at 350-375 km away from the inherited structure, which would be well below the Greenland craton, and 4) the timing of the two break-up branches only 5-10 Myr apart in the model, that corresponds well to the 64 Ma for the Labrador Sea ('plume-centered' break-up branch) and 7 Myr later, at 57 Ma the Aegir Ridge ('structural inherited' break-up branch). We note that given the natural limitations of the used 2D approach, further explore the effect of plume on multi-branch systems with 3D tests would facilitate a more detailed comparison with observations in the North Atlantic.

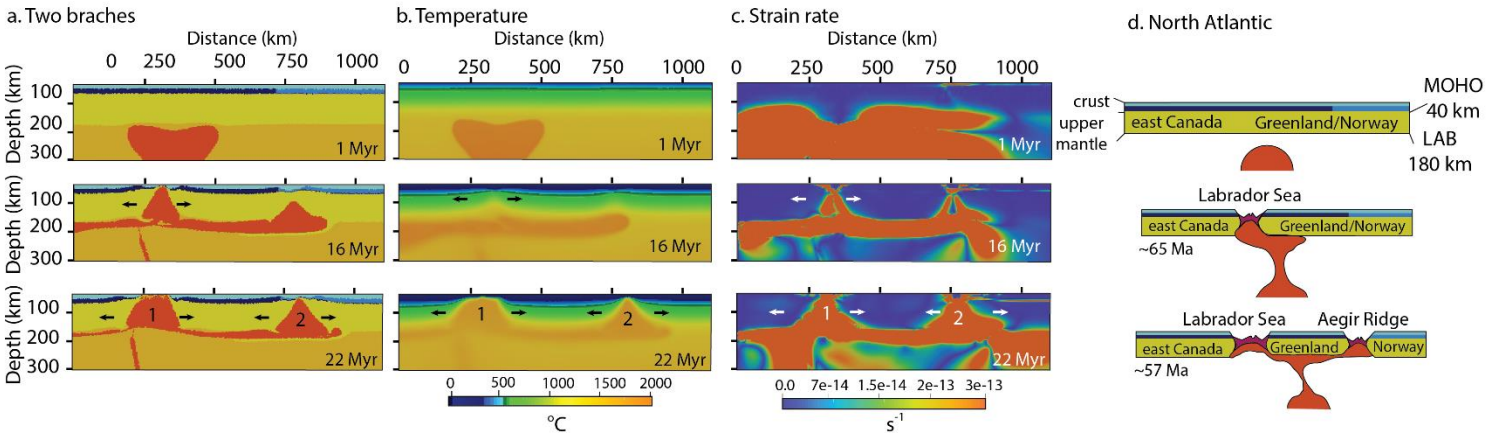

Figure 4. Phase (a), temperature (b) and strain rate (c) plots of model 7 (Moho temperature of 500 °C, extensional rate of 10 mm/y, plume shift of 375 km). This model develops a "two-branch" break-up mode and bears strong similarities with the geodynamical evolution in the North Atlantic domain (d, schematic representation) : 1) the first branch forms in the left part of the model, corresponding to the strong crust, similar to Greenland craton that will eventually separate Greenland and Canada [*Peace et al.*, 2016]; 2) the second branch forms 6 million years later close the inherited structure, comparable to the break-up of the Caledonian orogeny eventually separating Greenland and Norway [*Lundin and Doré*, 2002]. The pink color on the schematic profiles refers to newly formed oceanic lithosphere.

Based on our modeling results and examples from nature, we note that rheological heterogeneities in the lithosphere, its thermal state and acting mechanical forces and the lithospheric structure are important parameters for the rift-to-break-up evolution of the system. In addition we show that, the initial location of the plume with respect to a laterally varying lithosphere is not only an important factor on rift and break-up modes and geometries, but also affects the timing and order of the development of the branches. We argue that, in combination with far-field forces and the thermal state of the system, the emplacement of the plume anomaly is a key parameter for plume-induced continental rifting and break-up numerical modeling.

5. Acknowledgment

This study is co-funded by the Advanced ERC Grant 290864 RHEOLITH to Alexander Koptev. Anouk Beniest is funded by IFP Energies nouvelles. The numerical simulations were performed on the ERC-Rheolith funded SGI Ulysse cluster of ISTeP. We thank Taras Gerya for providing the numerical code I3ELVIS. The figures in the supporting material contain the numerical simulation data.

6. References

Abdelmalak, M. M., S. Planke, J. I. Faleide, D. A. Jerram, D. Zastrozhnov, S. Eide, and R. Myklebust (2016), The development of volcanic sequences at rifted margins: new insights from the structure and morphology of the Vøring Escarpment, mid-Norwegian Margin, *J. Geophys. Res. Solid Earth*, *121*(7), 5212–5236, doi:10.1002/2015JB012788.

Bellahsen, N., C. Faccenna, F. Funiciello, J. M. Daniel, and L. Jolivet (2003), Why did Arabia separate from Africa? Insights from 3-D laboratory experiments, *Earth Planet. Sci. Lett.*, *216*, 365–381, doi:10.1016/S0012-821X(03)00516-8.

Beniest, A., A. Koptev, and E. Burov (2017), Numerical models for continental break-up: Implications for the South Atlantic, *Earth Planet. Sci. Lett.*, *461*, 176–189, doi:10.1016/j.epsl.2016.12.034.

Bittner, D., and H. Schmeling (1995), Numerical modelling of melting processes and induced diapirism in the lower crust, *Geophys. J. Int.*, *123*, 59–70.

Brun, J.-P. (2002), Deformation of the continental lithosphere: Insights from brittle-ductile models, *Geol. Soc. London, Spec. Publ.*, *200*(1), 355–370, doi:10.1144/GSL.SP.2001.200.01.20.

Brune, S., A. A. Popov, and S. V Sobolev (2013), Quantifying the thermo-mechanical impact of plume arrival on continental break-up, *Tectonophysics*, *604*, 51–59, doi:10.1016/j.tecto.2013.02.009.

Brune, S., C. Heine, M. Pérez-Gussinyé, and S. V Sobolev (2014), Rift migration explains continental margin asymmetry and crustal hyper-extension, *Nat. Commun.*, *5*(4014), 1–9, doi:10.1038/ncomms5014.

Buck, W. R. (2007), Dynamic Processes in Extensional and Compressional Settings: The Dynamics of Continental Breakup and Extension, *Treatise Geophys.*, *6*, 335–376, doi:10.1016/B978-044452748-6.00110-3.

Burov, E., and S. Cloetingh (2010), Plume-like upper mantle instabilities drive subduction initiation, *Geophys. Res. Lett.*, *37*(3), 1–6, doi:10.1029/2009GL041535.

Burov, E., and T. Gerya (2014), Asymmetric three-dimensional topography over mantle plumes, *Nature*,

335 *513*, 85–89, doi:10.1038/nature13703.
336 Burov, E. B. (2011), Rheology and strength of the lithosphere, *Mar. Pet. Geol.*, *28*, 1402–1443,
337 doi:10.1016/j.marpetgeo.2011.05.008.
338 Chalmers, J. A., L. M. Larsen, and A. K. Pedersen (1995), Widespread Palaeocene volcanism around the
339 northern North Atlantic and Labrador Sea: evidence for a large, hot, early plume head, *J. Geol. Soc.*
340 *London*, *152*(1992), 965–969.
341 Chenin, P., and C. Beaumont (2013), Influence of offset weak zones on the development of rift basins:
342 Activation and abandonment during continental extension and breakup, *J. Geophys. Res. Solid*
343 *Earth*, *118*(4), 1698–1720, doi:10.1002/jgrb.50138.
344 Clauser, C., and E. Huenges (1995), Thermal Conductivity of Rocks and Minerals, *Rock Phys. Phase*
345 *Relations A Handb. Phys. Constants, ref. Shelf 3*, 105–126.
346 Connolly, J. A. D. (2005), Computation of phase equilibria by linear programming : A tool for
347 geodynamic modeling and its application to subduction zone decarbonation, *Earth Planet. Sci. Lett.*,
348 *236*, 524–541, doi:10.1016/j.epsl.2005.04.033.
349 Coulié, E., X. Quidelleur, P. Gillot, V. Courtillot, J.-C. Lefèvre, and S. Chies (2003), Comparative K - Ar
350 and Ar / Ar dating of Ethiopian and Yemenite Oligocene volcanism : implications for timing and
351 duration of the Ethiopian traps, *Earth Planet. Sci. Lett.*, *206*, 477–492.
352 D'Acremont, E., S. Leroy, and E. B. Burov (2003), Numerical modelling of a mantle plume: the plume
353 head–lithosphere interaction in the formation of an oceanic large igneous province, *Earth Planet.*
354 *Sci. Lett.*, *206*, 379–396, doi:10.1016/S0012-821X(02)01058-0.
355 Davaille, A., E. Stutzmann, G. Silveira, J. Besse, and V. Courtillot (2005), Convective patterns under the
356 Indo-Atlantic « box », *Earth Planet. Sci. Lett.*, *239*(3–4), 233–252, doi:10.1016/j.epsl.2005.07.024.
357 Davies, D. R., N. Rawlinson, G. Iaffaldano, and I. H. Campbell (2015), Lithospheric controls on magma
358 composition along Earth's longest continental hotspot track, *Nature*, *525*(7570), 511–514,
359 doi:10.1038/nature14903.
360 Ernesto, M., L. S. Marques, E. M. Piccirillo, E. C. Molina, N. Ussami, P. Comin-Chiaramonti, and G.
361 Bellinie (2002), Paraná Magmatic Province- Tristan da Cunha plume system: fixed versus mobile
362 plume, petrogenetic considerations and alternative heat sources, *J. Volcanol. Geotherm. Res.*, *118*,
363 15–36.
364 French, S. W., and B. Romanowicz (2015), Broad plumes rooted at the base of the Earth's mantle beneath
365 major hotspots, *Nature*, *525*(7567), 95–99, doi:10.1038/nature14876.
366 Gaina, C., W. R. Roest, R. D. Müller, and P. Symonds (1998), The Opening of the Tasman Sea: a gravity
367 anomaly animation, *Earth Interact.*, *2*(4), 1–23.
368 Gaina, C., L. Gernigon, and P. Ball (2009), Palaeocene – Recent plate boundaries in the NE Atlantic and

the formation of the Jan Mayen microcontinent, *J. Geol. Soc. London*, *166*, 601–616, doi:10.1144/0016-76492008-112.

Gerya, T. (2010), Dynamical instability produces transform faults at mid-ocean ridges, *Science*, *329*(5995), 1047–1050.

Gerya, T. V, and D. A. Yuen (2007), Robust characteristics method for modelling multiphase visco-elasto-plastic thermo-mechanical problems, *Phys. Earth Planet. Inter.*, *163*, 83–105, doi:10.1016/j.pepi.2007.04.015.

Greenhalgh, E. E., and N. J. Kusznir (2007), Evidence for thin oceanic crust on the extinct Aegir Ridge, Norwegian Basin, NE Atlantic derived from satellite gravity inversion, *Geophys. Res. Lett.*, *34*, 1–5, doi:10.1029/2007GL029440.

Hofmann, C., V. Courtillot, G. Féraud, P. Rochette, G. Yirgu, E. Ketefo, and R. Pik (1997), Timing of the Ethiopian flood basalt event and implications for plume birth and global change, *Nature*, *389*, 838–841, doi:10.1038/39853.

Huismans, R. S., and C. Beaumont (2008), Complex rifted continental margins explained by dynamical models of depth-dependent lithospheric extension, *Geology*, *36*(2), 163–166, doi:10.1130/G24231A.1.

Huismans, R. S., Y. Y. Podladchikov, and S. Cloetingh (2001), Transition from passive to active rifting: relative importance of asthenospheric doming and passive extension of the lithosphere, *J. Geophys. Res.*, *106*(B6), 11271–1191.

Kerr, A., J. Hall, R. J. Wardle, C. F. Gower, and B. Ryan (1997), Early Proterozoic Belts Ketilidian, *Tetonics*, *16*(6), 942–965.

Kohlstedt, D. L., B. Evans, and S. J. Mackwell (1995), Strength o the lithosphere: constraints imposed by laboratoy experiments, *J. Geophys. Res.*, *100*(B9), 17,587-17,602.

Koptev, A., E. Calais, E. Burov, S. Leroy, and T. Gerya (2015), Dual continental rift systems generated by plume – lithosphere interaction, *Nat. Geosci.*, *8*, 388–392, doi:10.1038/NGEO2401.

Koptev, A., E. Burov, E. Calais, S. Leroy, T. Gerya, L. Guillou-Frottier, and S. Cloetingh (2016), Contrasted continental rifting via plume-craton interaction: Applications to Central East African Rift, *Geosci. Front.*, *7*, 221–236, doi:10.1016/j.gsf.2015.11.002.

Koptev, A., E. Burov, T. Gerya, L. Le, S. Leroy, E. Calais, and L. Jolivet (2017), Plume-induced continental rifting and break-up in ultra-slow extension context: Insights from 3D numerical modeling, *Tectonophysics*, 1–17, doi:10.1016/j.tecto.2017.03.025.

Larsen, H. C., and A. D. Saunders (1998), Tectonism and volcanism at the southeast Greenland rifted margin: a record of plume impact and later continental rupture, *Proc. Ocean Drill. Progr. Sci. Results*, *152*, 503–533, doi:10.2973/odp.proc.sr.152.1998.

Lavecchia, A., C. Thieulot, F. Beekman, S. Cloetingh, and S. Clark (2017), Lithosphere erosion and continental breakup: Interaction of extension, plume upwelling and melting, *Earth Planet. Sci. Lett.*, *467*, 89–98, doi:10.1016/j.epsl.2017.03.028.

Lavier, L. L., and G. Manatschal (2006), A mechanism to thin the continental lithosphere at magma-poor margins, *Nature*, *440*(7082), 324–328, doi:10.1038/nature04608.

Lundin, E., and A. G. Doré (2002), Mid-Cenozoic post-breakup deformation in the "passive" margins bordering the Norwegian - Greenland Sea, *Mar. Pet. Geol.*, *19*, 79–93.

Manatschal, G., L. Lavier, and P. Chenin (2015), The role of inheritance in structuring hyperextended rift systems: Some considerations based on observations and numerical modeling, *Gondwana Res.*, *27*(1), 140–164, doi:10.1016/j.gr.2014.08.006.

McClusky, S. et al. (2010), Kinematics of the southern Red Sea – Afar Triple Junction and implications for plate dynamics, *Geophys. Res. Lett.*, *37*(L05301), 1–5, doi:10.1029/2009GL041127.

Mohriak, W. U., M. Nóbrega, M. E. Odegard, B. S. Gomes, and W. G. Dickson (2010), Geological and geophysical interpretation of the Rio Grande Rise, south-eastern Brazilian margin: extensional tectonics and rifting of continental and oceanic crusts, *Pet. Geosci.*, *16*, 231–245, doi:10.1144/1354-079309-910.

Moulin, M., D. Aslanian, and P. Unternehr (2010), A new starting point for the South and Equatorial Atlantic Ocean, *Earth-Science Rev.*, *98*, 1–37, doi:10.1016/j.earscirev.2009.08.001.

Peace, A., K. McCaffrey, J. Imber, J. Phethean, G. Nowell, K. Gerdes, and E. Dempsey (2016), An evaluation of Mesozoic rift-related magmatism on the margins of the Labrador Sea: Implications for rifting and passive margin asymmetry, *Geosphere*, *12*(6), 1–24, doi:10.1130/GES01341.1.

Ranalli, G. (1995), *Rheology of the Earth, 2nd edition*, Chapmann and Hall, 413 pp.

Rickers, F., A. Fichtner, and J. Trampert (2013), The Iceland-Jan Mayen plume system and its impact on mantle dynamics in the North Atlantic region: Evidence from full-waveform inversion, *Earth Planet. Sci. Lett.*, *367*, 39–51, doi:10.1016/j.epsl.2013.02.022.

Rogozhina, I., A. G. Petrunin, A. P. M. Vaughan, B. Steinberger, J. V Johnson, M. K. Kaban, R. Calov, F. Rickers, M. Thomas, and I. Koulakov (2016), Melting at the base of the Greenland ice sheet explained by Iceland hotspot history, *Nat. Geosci.*, *9*, 366–369, doi:10.1038/NGEO2689.

Saunders, A. D., J. G. Fitton, A. C. Kerr, M. J. Norry, and R. W. Kent (1997), The North Atlantic igneous province, *Geophys. Monogr.*, *100*, 45–93.

Schellart, W. P. (2004), Quantifying the net slab pull force as a driving mechanism for plate tectonics, *Geophys. Res. Lett.*, *31*(7), 10–14, doi:10.1029/2004GL019528.

Schlömer, A., W. H. Geissler, W. Jokat, and M. Jegen (2017), Hunting for the Tristan mantle plume - An upper mantle tomography around the volcanic island of Tristan da Cunha, *Earth Planet. Sci. Lett.*,

462, 122–131, doi:10.1016/j.epsl.2016.12.028.

Skogseid, J., S. Planke, J. I. Faleide, T. Pedersen, O. Eldholm, and F. Neverdal (2000), NE Atlantic continental rifting and volcanic margin formation, *Geol. Soc. London, Spec. Publ.*, *167*, 295–326.

Torsvik, T. H., S. Rousse, C. Labails, and M. A. Smethurst (2009), A new scheme for the opening of the South Atlantic Ocean and the dissection of an Aptian salt basin, *Geophys. J. Int.*, *177*, 1315–1333, doi:10.1111/j.1365-246X.2009.04137.x.

Torsvik, T. H. et al. (2015), Continental crust beneath southeast Iceland, *Proc. Natl. Acad. Sci.*, *112*(5), E1818–E1827, doi:10.1073/pnas.1423099112.

Turcotte, D. L., and G. Schubert (2002), *Geodynamics*, Cambridge Univ. Press, Cambridge, UK.

Zhao, D. (2007), Seismic images under 60 hotspots: Search for mantle plumes, *Gondwana Res.*, *12*, 335–355, doi:10.1016/j.gr.2007.03.001.